Available online at www.sciencedirect.com
ScienceDirect
Pattern Recognition Letters 28 (2007) 286–292
Pattern Recognition Letters
www.elsevier.com/locate/patrec

Multiresolution mammogram analysis in multilevel decomposition

Essam A. Rashed [a,*], Ismail A. Ismail [b], Sherif I. Zaki [a]

[a] Department of Mathematics, Faculty of Science, Suez Canal University, Ismailia 41522, Egypt
[b] Department of Computer Science, Faculty of Computers and Informatics, Zagazig University, Zagazig, Egypt

Received 5 February 2005; received in revised form 5 November 2005
Available online 7 September 2006

Communicated by C.-F. Westin

Abstract

A multiresolution analysis system for interpreting digital mammograms is proposed and tested. This system is based on using fractional amount of biggest wavelets coefficients in multilevel decomposition. A set of real labeled database is used in evaluating the proposed system. The evaluation results show that the system has a remarkably high efficiency compared by other systems known till present especially in the area of distinguishing between benign and malignant tumors.

Keywords: Digital mammogram; Discrete wavelets transform; Features extraction; Breast cancer diagnosis

1. Introduction

Breast cancer is one of the most dangerous types of cancer among women all over the world. Early detection of breast cancer is essential in reducing life fatalities (Pisani et al., 1993). However, achieving this early detection of the cancer is not an easy task. Although that the most accurate detection method in the medical environment is biopsy; it is an aggressive invasive procedure that involves some risks, patient discomfort and high cost. Moreover, there is a high percent of negative cases (70–90%) where breast biopsies were performed unnecessarily (Meyer et al., 1990). Therefore, digital mammography has been used in attempts to reduce the negative biopsy ratio and the cost to society by improving feature analysis and refining criteria for recommendation for biopsy (Sickles, 1991). Digital mammography is a convenient and easy tool in classifying tumors and many applications in the literature prove its effective use in breast cancer diagnosis (e.g. Mudigonda et al., 2000, 2001).

Image features extraction is an important step in the preprocessing of signal processing techniques. The features of digital image could be extracted directly from the spatial data or from a different space. Using a different space by special data transform such as Fourier transform or wavelets transform could be helpful to separate a special data that contain specific characteristics. Detecting the features of image texture is a difficult process because these features (or this texture) are mostly variable and scale-dependent.

Designing an effective diagnosis system for digital mammograms is still a challenging problem that needs more investigation. Two main functions should be included in such a system; the first is to distinguish between the normal tissues and the different types of tumors such as microcalcification clusters, spiculated lesions, circumscribed masses, ill-defined lesions. The second function is to differentiate between benign and malignant tumors. Mammogram features extraction is widely studied from the side of pattern recognition analysis to detect the best features that could represent mammogram. This is a difficult task due to the irregularity of mammograms texture. The shortage of diagnosis using mammograms is mostly due to human factor as the abnormality indicators are varied in shape, size, and

* Corresponding author. Tel.: +20 10 680 9031; fax: +20 643 356 416.
E-mail addresses: essam@khawarizmi.com, essam.rashed@gmail.com (E.A. Rashed).

0167-8655/$ - see front matter © 2006 Elsevier B.V. All rights reserved.
doi:10.1016/j.patrec.2006.07.010

brightness. Also, vessels and muscles could be confused parameters as they appear in similar shapes of tumors. The most common shortage is the unclearly distinguish between the benign and malignant lesions (Sickles, 2000).

In this paper, an effective supervised classifier for mammograms is proposed using the discrete wavelet transform decomposition. The achieved numerical results indicate the effectiveness of the classifier in solving three basic problems in mammogram diagnosis:

1. Classification of cancerous versus cancerous-free patterns.
2. Classification of abnormality indicator (i.e. microcalcifications, circumscribed masses, spiculated lesions, and ill-defined masses).
3. Classification of risk level of cancerous cells (i.e. benign versus malignant).

This paper consists of five sections, Section 1 contains this introduction, Section 2 discusses the properties of typical mammogram and its classes and a literature review of most recent work in mammogram classifications. The main problem discussion and a multiresolution approach are presented in Section 3. The achieved numerical results are presented and discussed in Section 4 while Section 5 contains the conclusion and future work.

2. Digital mammograms

The mammogram is acquired by compressing the patient breast between two acrylic plates while an X-ray signal is emitted through. A typical mammogram is a gray scale image that indicates the details inside the patient breast by meaning of contrast. These details could be normal tissues, vessels, muscles, different types of masses, and noise.

Each type of masses has different properties of shape, size, distribution, and brightness which act as features that help the radiologist to effectively diagnosis the breast tumors. This means that the experience of the radiologist and the image quality are the main important factors in this manual classification. Microcalcifications are small groups of calcified cells that have a long scale in form, size and distribution. Circumscribed masses mostly appear as uniform and smooth masses in the shape of irregular circles. Spiculated lesions appear as a region with segments distributed in many directions as a multi-arms star. Ill-defined masses do not have a fixed pattern (Liu et al., 2001). Fig. 1 shows some examples to these features.

Another diagnosis classification that needs to be investigated is to check the dangerous level of cancerous cells which can be either benign or malignant. In some cases, there were no exact difference in shape between benign and malignant lesions and they could be identified only using biopsy. This ranks the computerized solution of this problem as important contribution in mammogram diagnosis.

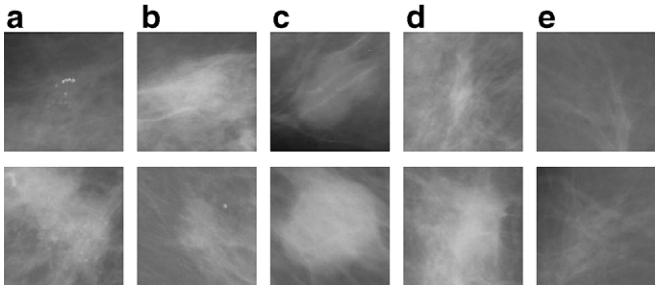

Fig. 1. Sample of mammograms used: (a) microcalcification clusters up benign (mdb019) and down malignant (mdb209), (b) ill-defined masses up benign (mdb032) and down malignant (mdb058), (c) circumscribed masses up benign (mdb005) and down malignant (mdb028), (d) spiculated lesions up benign (mdb145) and down malignant (mdb178), (e) normal tissues (*tumor free*) up (mdb006) and down (mdb009).

In the present study, a set of images that are provided by the Mammographic Image Analysis Society (MIAS [1]) are used in applying the new diagnosis technique. These images are previously investigated and labeled by an expert radiologist based on a technical experience and a biopsy. The original mammograms are 1024×1024 pixels. This database is selected according to the variety cases included and widely usage in similar research work. Table 1 illustrates the distribution of the selected images in our experiment. From the selected images a regions of interest (ROI's) are extracted with size of 128×128 pixels. Theses ROI's contain the abnormality centered. Fig. 1 shows that distinguishing different types or levels of abnormality by using visual properties is a very difficult task that contains a large scale of risk. This visual detection could be improved by using a double reading system. Pervious studies proved that using a computerized classification improves this visual classification with high successive rates (e.g. Mello-Thoms, 2003; Chan et al., 1990; Chen et al., 1999) However, designing a complete computerized classification system for digital mammogram is still a challenging problem and many researchers suggested different solutions to provide an optimum system; a survey is presented by Cheng et al. (2003). A review of the most recent solutions will be discussed in this section.

A wavelet based algorithm is proposed by Boccignone et al. (2000) for detecting the microcalcification clusters in digital mammogram. A thresholding technique was used to separate microcalcifications from the background texture. This technique was based on Renyi's entropy. They achieve successive results by applying it to Nijmegen mammogram data set. A computer-aided diagnosis (CAD) system was developed by Yu and Guan (2000) for automatic identification of microcalcification clusters in digitized mammogram films. In this system microcalcification pixels are segmented out using mixed features obtained from wavelet transform and gray level statistical analysis and labeled into potential individual microcalcification objects.

[1] http://peipa.essex.ac.uk/ipa/pix/mias/.

Table 1
The distribution of selected cases from MIAS database

	Norm	Calc		Circ		Ill		Spic		Total
		B	M	B	M	B	M	B	M	
Fty	66	02	04	10	02	02	05	02	03	96
Dns	76	05	05	03	0	01	01	05	02	98
Gld	65	05	04	06	02	03	02	04	03	94
Total	207	12	13	19	04	06	08	11	08	288

Class of abnormality present
Norm normal tissue
Calc microcalcification clusters
Circ circumscribed masses
Ill ill-defined masses
Spic spiculated lesions
Background tissue
Fty fatty
Gld fatty-glandular
Dns dense-glandular
Cancerous level
B benign
M malignant

Then, these individual microcalcification objects are classified as true or false individual microcalcification objects based on a set of 31 features. They achieve 90% mean true positive (TP) detection rate at the price of 0.5 false positive (FP) per image.

A CAD system designed by Kita et al. (2002) for estimating the 3D positions of lesions found in two mammographic views is described. The method calculates curved epipolar lines by developing a simulation of breast deformation into stereo camera geometry. Using such curved epipolar lines, not only can we determine point correspondences, but can estimate the 3D location of a lesion. The correctness of the 3D positions calculated by the system is examined using a set of breast lesions. Lee et al. (2003) present a shape recognition-based neural network built with universal feature planes, called Shape Cognitron (S-Cognitron) is introduced to classify clustered microcalcifications. The system is evaluated by using Nijmegen mammogram database and experimental results show that sensitivity and specificity can reach 86.1% and 74.1%, respectively. An approach for classifying clusters of microcalcifications is proposed by De Santo et al. (2003). This approach is based on a Multiple Expert System; such system aggregates several experts, some of which are devoted to classify the single microcalcifications while others are aimed to classify the cluster considered as a whole. The final output results from the suitable combination of the two groups of experts. The tests performed on a standard database of 40 mammogram images.

In their mammogram analysis study, Liu et al. (2001) proved that the use of multiresolution analysis of the mammograms improve the effectiveness of any diagnosis system based on wavelets coefficients. They use a set of statistical features with binary tree classifier in their diagnosis system. Later, Ferreira and Borges (2003) indicate that the use of the biggest wavelets coefficients in the low frequency coefficients of wavelets transform could be use as a signature vector for the corresponding mammogram. In their study they use Haar and Daubechies-4 wavelets with selection of 100, 200, 300, and 500 biggest wavelets coefficient. This approach is applied on some images selected from MIAS database. A ROI's of 64×64 pixels are selected from the original mammograms. Classification is done by measures the Euclidean distance between class prototype and desired mammogram coefficient vector. They achieve an interesting results classifying the lesion types and to distinguish between benign and malignant tumors (i.e. they reach 100% correct classification rate in some cases).

3. Multiresolution analysis and the new approach

Image texture is a confusing measurement that depends mainly on the scale in which the data are observed. Different types of image have different types of texture. Earlier studies proved that the texture of mammograms is an irregular texture. Accordingly, some measurements like entropy, energy, contrast and homogeneity could be improved when combined with a multiresolution domain transform. To design an automated mammogram classifier, an uncorrelated measurement needs to be investigated to transform the data into a different domain. The mammogram classifying problem needs a transform that can uncorrelate the data without losing the image main characteristics. These properties mean that discrete wavelets transform is the most suitable transform for mammograms features extraction.

The idea of wavelets that is explained in details by Daubechies (1992) who stated that wavelets are functions that are used as the basis to represent other functions. This one is called *mother wavelet*. A set of functions can be generated by translations and dilations of the mother function. Suppose that $\Psi(x)$ is a mother function, the translations and dilations will be $\Psi(\frac{x-b}{a})$, while $a \in \Re^+$and $b \in \Re$. The values of a and b can be calculated using $a = 2^{-j}$ and $b = k \cdot 2^{-j}$ while k and j are integers.

Wavelets decomposition is based on applying 2D wavelets transform to the image and a set of four different coefficients are produced in each level of decomposition. The produced coefficients are

- Low frequency coefficients (A).
- Vertical high frequency coefficients (V).
- Horizontal high frequency coefficients (H).
- High frequency coefficients in both directions (D).

Three levels of 2D wavelets decompositions are illustrated in Fig. 2. In this study, we use a four different levels of decompositions based on three different wavelets that are Daubechies-4, Daubechies-8, and Daubechies-16. In each level of decomposition, a percentage of the low frequency coefficients is used to represent the corresponding mammogram (i.e. feature vector). The idea of using a group of biggest coefficients is previously presented by Ferreira and Borges (2003). This idea is extended here

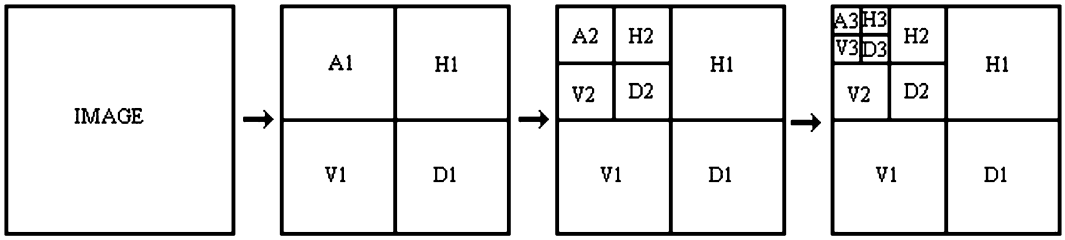

Fig. 2. Wavelets multiresolution decomposition.

not only by testing a fixed amount of values but also by covering all possible rates (10–90%) of low frequency coefficients that may contribute positively to the classification rate. Another idea implemented here was previously discussed by Liu et al. (2001) and extended here by applying multilevel wavelet decomposition, exactly four levels of decomposition. In conclusion, two main ideas are explored in this paper. The first idea is using fractions of wavelets coefficients as a signature vector and the second idea is applying this in different levels of decompositions.

A set of 288 ROI's that are extracted from one original mammogram from MIAS database are used to test the new algorithm. The Euclidean distance is used to design the classifier that is based on calculating the distance between the feature vectors and the class core vector. The system automatically classifies the feature vector to a diagnosis class C_{diag} by finding the nearest class to this vector. This is done by testing the distance between this feature vector and all class core vectors. Class core vectors are previously calculated using a set of specific class ROI's. The following equations describe the classification method.

$$\text{Dist}(A, C_{\text{diag}}) = \text{MinDist}, \tag{1}$$

$$\text{MinDist} = \min_{1 \leqslant m \leqslant M} (\text{Dist}(A, C_m)), \tag{2}$$

$$\text{Dist}(A, C_m) = \frac{1}{J} \sum_{j=1}^{J} \sum_{i=1}^{L^j} \sqrt{(A^j(i) - C_m^j(i))^2}, \quad 1 \leqslant m \leqslant M. \tag{3}$$

While A^j is the coefficient vector of the jth decomposition level for diagnosis image, C_m^j is the class core vector for class m at decomposition level j, L^j is the length of coefficient

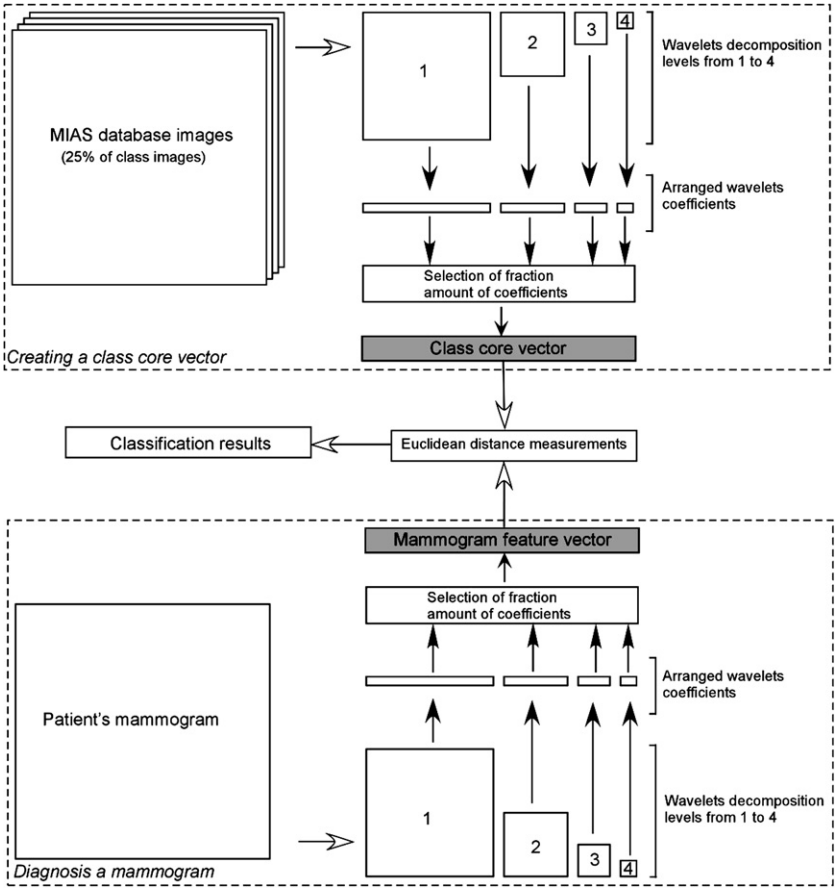

Fig. 3. The multiresolution mammogram diagnosis system.

Table 2
Successful rates of classification, in percentage with Daubechies-4, -8, -16 wavelets

Selected wavelet coefficients (%)	Daubechies-4					Daubechies-8					Daubechies-16				
	Spic	Circ	Calc	Ill	Norm	Spic	Circ	Calc	Ill	Norm	Spic	Circ	Calc	Ill	Norm
10	84.2	47.8	52	78.6	96.1	89.5	87	72	85.7	96.6	84.2	65.2	64	71.4	87
20	100	82.6	48	85.7	88.9	100	78.3	80	100	92.3	94.7	82.6	76	71.4	82.1
30	94.7	95.7	64	71.4	99.5	89.5	100	80	100	99	100	91.3	76	78.6	99.5
40	63.2	91.3	76	57.1	96.6	57.9	95.7	96	92.9	100	93.2	100	76	64.3	93.2
50	68.4	39.1	100	64.3	89.4	73.7	60.9	100	78.6	100	68.4	47.8	96	92.9	88.9
60	73.7	56.5	92	50	79.2	78.9	60.9	88	57.1	99.5	73.7	52.2	92	85.7	83.6
70	78.9	65.2	88	92.9	84.1	84.2	65.2	80	78.6	85.5	89.5	65.2	72	100	90.3
80	89.5	82.6	92	85.7	85.5	100	87	72	78.6	90.3	84.2	91.3	72	85.7	58.9
90	84.2	82.6	80	57.1	91.3	94.7	78.3	76	85.7	98.1	78.9	73.9	68	57.1	69.1

Table 3
Successful rates of classification, in percentage with Daubechies-4, -8, -16 wavelets

Selected wavelet coefficients (%)	Daubechies-4		Daubechies-8		Daubechies-16	
	Benign	Malignant	Benign	Malignant	Benign	Malignant
10	83.3	84.8	97.9	84.8	100	84.8
20	93.8	81.8	100	81.8	95.8	51.5
30	100	84.8	100	78.8	91.7	81.8
40	89.6	84.8	97.9	81.8	91.7	87.9
50	87.5	87.9	95.8	90.9	89.6	90.9
60	87.5	93.9	93.8	51.5	87.5	93.9
70	87.5	100	91.7	100	85.4	97
80	85.4	93.9	91.7	100	87.5	100
90	64.6	97	93.8	87.9	87.5	93.9

vector at decomposition level j, M is the number of classifications classes (equals 5 for tumor types diagnosis and 2 for risk level diagnosis), and J is the number of decomposition levels used (here $J = 4$).

The class core vector for each decomposition level C_m^j is previously calculated using a set of 25% of class ROI's randomly selected from the dataset using the following equation:

$$C_m^j = \frac{1}{N^j} \sum_{n=1}^{N^j} \sum_{i=1}^{L^j} A_m^j(i), \quad 1 \leqslant m \leqslant M, \tag{4}$$

where N^j is the number of selected ROI's to produce the class core vector at decomposition level j, and A_m^j is the coefficient vector for ROI's for the class m at decomposition level j.

The images that are used in testing the effectiveness of the proposed system are decomposed into four level of decomposition using Daubechies-4, -8, -16 wavelets. In each experiment, a class core vector is calculated for each class using Eq. (4) then all the ROI's extracted from the MIAS database is used in the test phase including those used to produce the class core vectors. Eq. (3) is used to measure the distance between the coefficient vector A and all available classes' core vectors. This done by find the average mean for a four distances measured in the four decomposition levels. The system is diagnosis the coefficient vector to a specific class using Eqs. (1) and (2). Fig. 3 illustrates the steps of creating the class core vectors and also the similar steps of diagnosis mammogram image.

4. Results and comments

In the practical experiment, two main problems are covered, to distinguish between the types of tumors according to the physical properties and to classify these tumors according to the level of risk. In the first problem, five classes are used as main classes that are microcalcifications, spiculated lesions, circumscribed lesions, ill-defined lesions, and normal tissues. The second problem consists of two main classes that are benign and malignant tumors.

The Daubechies-4, Daubechies-8, and Daubechies-16 wavelets are used in the decomposition process while Rice Wavelets Toolbox [2] is used to apply the wavelets transform process. In each class, four levels of decompositions are applied, and then a fractional percent of the biggest coefficients is used to be the feature vector of the corresponding mammogram. Table 2 shows the successful classification rate during using Daubechies-4, -8, -16 in all different fractions of coefficients used for solving the first problem.

From the results in Table 2, using Daubechies-4 wavelets, a 100% successful classifying rate is reached in spiculated lesions when a set of 20% of coefficients is used. For circumscribed lesions 95.7% of classification rate is achieved using 30% of the coefficients. In microcalcification, a 100% rate is achieved when 50% of the coefficients are used to measure the distance, while ill-defined lesion peaks at 70% of the coefficients and scores 92.9%. The

[2] <http://www.dsp.rice.edu/software>.

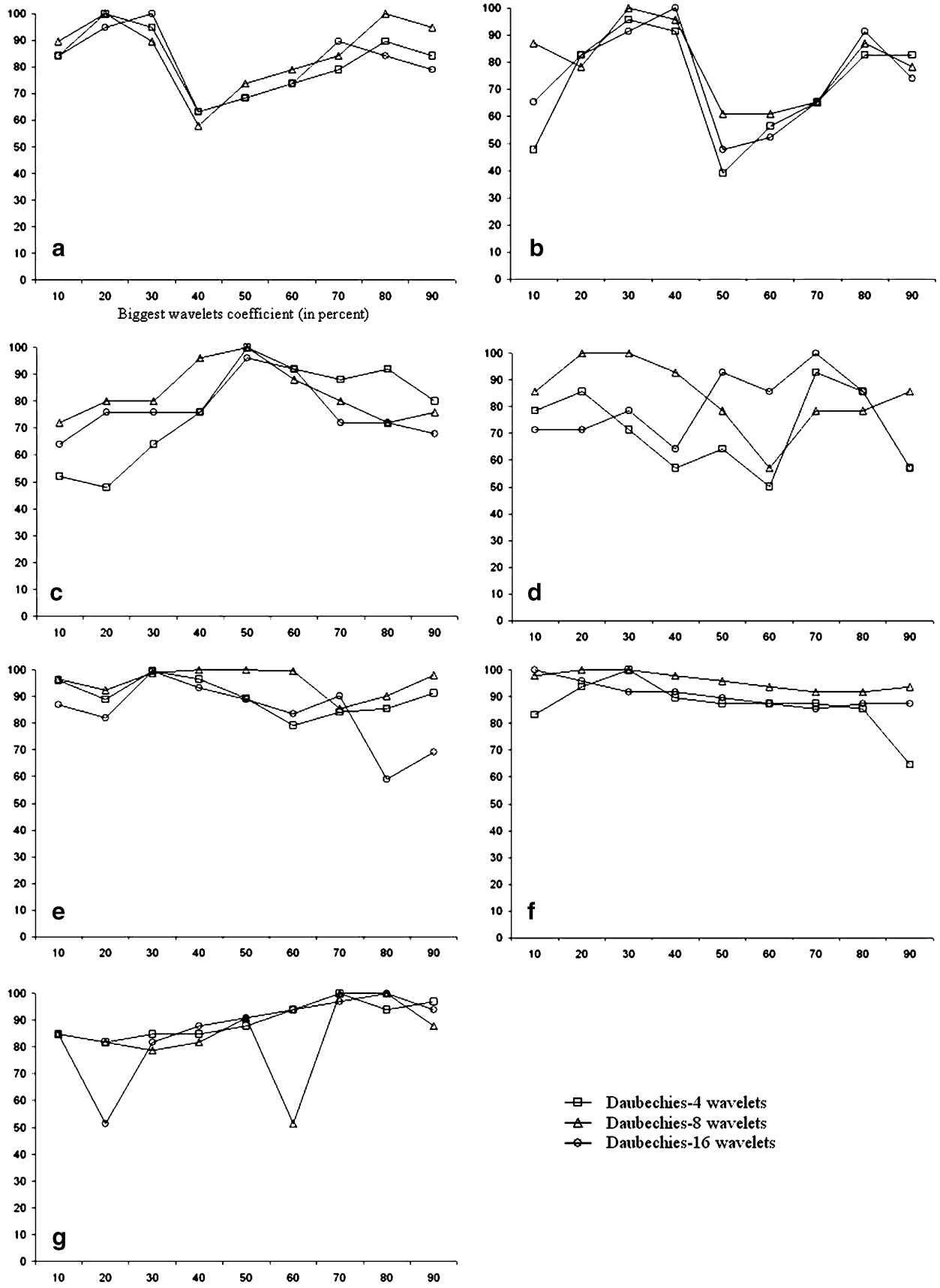

Fig. 4. Diagnosis results for all classes: (a) spiculated lesions, (b) circumscribed masses, (c) microcalcification clusters, (d) ill-defined masses, (e) normal tissues (mass-free), (f) benign lesions, (g) malignant lesions.

normal tissue mammograms achieve the maximum successful classification rate (99.5%) when 30% of the coefficients are used.

Daubechies-8 shows slightly better results than in Daubeshies-4. In spiculated lesions, it achieves two peak points at 20% and 80% of the coefficients, while circumscribed lesions reach full successful classification rate 100% at 30%. Microcalcifications peak is still record 100% at the same point 50% while ill-defined lesion records a rate of 100% at 20% and 30%. The normal tissue achieve 100% peak at two points 40% and 50%. When Daubechies-16 is used spiculated lesions achieve 100% peak point at 30% of the coefficients values, while circumscribed lesions reach rate of 100% at 40%. Microcalcifications peak is reduced to 96% at the same point 50% of the coefficients, while ill-defined lesion record 100% rate at 70%. The normal tissue achieve 99.5% successful classification rate when 30% of the coefficients are used.

From these results it can be concluded that using Dabechies-8 produces the most significantly correct classification rates. Spiculated lesions are classified better in the first quarter of biggest coefficients. Circumscribed lesions, microcalcification, and normal tissues achieve most accurate successful classifications within the second quarter of selected coefficients. No fixed range could be detected for the ill-defined lesions; this may be due to their wide range of shapes. The results illustrated in Table 3 shows the classification rate when using Daubechies-4, -8, and -16 wavelets for detecting the risk level of ROI's. It is clear from the tables that benign lesions achieve the best results in the second quarter and malignant ones in the last quarter. It is also clear that Daubechies-8 is still the most successful choice of wavelets. A summary of these results is shown in Fig. 4.

5. Conclusions and future work

Digital mammogram diagnosis is a practical field of investigation and positive results could effect the human being life preventing. In this study, a novel model is proposed by gathering two main concepts proved earlier; the concept of using biggest wavelets coefficients as a feature vector and the idea of using multiresolution analysis in mammograms features extraction. Experiment is applied on real labeled data and results show promising use of this technique and flexibility of modifying. The results are enhanced compared to those presented by Ferreira and Borges (2003). We believe that this positive enhancement is occurring as a result of using multilevel of wavelets decomposition analysis. The results also marks a special area of the wavelets coefficients that could high percent of successive indicates each class of tumors (e.g. spiculated lesions are correctly diagnosis within the first quarter of biggest wavelets coefficients). Future steps could include many distinct modifications; the effect of using other wavelets rather than Daubechies could be tested, the change of the coefficients groups (i.e. using H, L, or D) could be traced, and extended the number of decomposition levels. All these factors could affect positively or negatively to the results we achieved here.

References

Boccignone, G., Chianese, A., Picariello, A., 2000. Computer aided detection of microcalcifications in digital mammograms. Comput. Biol. Med. 30, 267–286.

Chan, H.-P., Sahiner, B., Helvie, M.A., Petrick, N., Roubidoux, M.A., Wilson, T.E., Alder, D.D., Paramagul, C., Newman, J.S., Sanjay-Gopal, S., 1990. Improvement of radiologists characterization of mammographic masses by using computer-aided diagnosis: An ROC study. Radiology 212, 817–827.

Chen, D.-R., Chang, R.-F., Huang, Y.-L., 1999. Computer-aided diagnosis applied to US of solid breast nodules by using neural networks. Radiology 213, 407–412.

Cheng, H.D., Cai, X., Chen, X., Hu, L., Lou, X., 2003. Computer-aided detection and classification of microcalcifications in mammograms: A survey. Pattern Recognition 36 (12), 2967–2991.

Daubechies, I., 1992. Ten lectures on wavelets. SIAM CBMS-NSF Series on Applied Mathematics, vol. 61. SIAM.

De Santo, M., Molinara, M., Tortorella, F., Vento, M., 2003. Automatic classification of clustered microcalcifications by a multiple expert system. Pattern Recognition 36, 1467–1477.

Ferreira, C.B.R., Borges, D.L., 2003. Analysis of mammogram classification using a wavelet transform decomposition. Pattern Recognition Lett. 24, 973–982.

Kita, Y., Tohno, E., Highnam, R.P., Brady, M., 2002. A CAD system for the 3D location of lesions in mammograms. Med. Image Anal. 6, 267–273.

Lee, S.-K., Chung, P.-C., Chang, C.-I., Lo, C.-S., Lee, T., Hsu, G.-C., Yang, C.-W., 2003. Classification of clustered microcalcifications using a shape cognitron neural network. Neural Networks 16, 121–132.

Liu, S., Babbs, C.F., Delp, E.J., 2001. Multiresolution detection of spiculated lesions in digital mammograms. IEEE Trans. Image Process. 10 (6), 874–884.

Mello-Thoms, C., 2003. Perception of breast cancer: Eye-position analysis of mammogram interpretation. Acad. Radiol. 10, 4–12.

Meyer, J.E., Eberlein, T.J., Stomper, P.C., Sonnenfeld, M.R., 1990. Biopsy of occult breast lesions: Analysis of 1261 abnormalities. J. Amer. Med. Assoc. 263, 2341–2343.

Mudigonda, N.R., Rangayyan, R.M., Leo Desautels, J.E., 2000. Gradient and texture analysis for the classification of mammographic masses. IEEE Trans. Med. Imaging 19 (10), 1032–1043.

Mudigonda, N.R., Rangayyan, R.M., Leo Desautels, J.E., 2001. Detection of breast masses in mammograms by density slicing and texture flow-field analysis. IEEE Trans. Med. Imaging 20 (12), 1215–1227.

Pisani, P., Parkin, D.M., Ferlay, J., 1993. Estimates of the worldwide mortality from eighteen major cancers in 1985: Implications for prevention and projections of future burden. Internat. J. Cancer 55, 891–903.

Sickles, E.A., 1991. Periodic mammographic follow-up of probably benign lesions: Results in 3,184 consecutive cases. Radiology 179, 463–468.

Sickles, E.A., 2000. Breast imaging: From 1965 to the present. Radiology 215, 1–16.

Yu, S., Guan, L., 2000. A CAD system for the automatic detection of clustered microcalcifications in digitized mammogram films. IEEE Trans. Med. Imaging 19 (2), 115–126.